Atmospheric Environment 98 (2014) 402–409

Contents lists available at ScienceDirect

Atmospheric Environment

journal homepage: www.elsevier.com/locate/atmosenv

Indicators to support the dynamic evaluation of air quality models

P. Thunis [a, *], A. Clappier [b]

[a] European Commission, JRC, Institute for Environment and Sustainability, Air and Climate Unit, Via E. Fermi 2749, 21027 Ispra, VA, Italy
[b] Université de Strasbourg, Laboratoire Image Ville Environnement, 3, Rue de l'Argonne, 67000 Strasbourg, France

HIGHLIGHTS

- Proposed indicators to evaluate air quality models for dynamic evaluation.
- Proposed diagram to evaluate emission reduction impacts on concentrations.
- Assessment of the robustness and non-linearity of model responses.
- Diagram and indicators are useful for policy-maker and model developers.

ARTICLE INFO

Article history:
Received 24 February 2014
Received in revised form
2 September 2014
Accepted 5 September 2014
Available online 6 September 2014

Keywords:
Dynamic evaluation
Air quality modeling
Performance indicators

ABSTRACT

Air quality models are useful tools for the assessment and forecast of pollutant concentrations in the atmosphere. Most of the evaluation process relies on the "operational phase" or in other words the comparison of model results with available measurements which provides insight on the model capability to reproduce measured concentrations for a given application. But one of the key advantages of air quality models lies in their ability to assess the impact of precursor emission reductions on air quality levels. Models are then used in a dynamic mode (i.e. response to a change in a given model input data) for which evaluation of the model performances becomes a challenge.

The objective of this work is to propose common indicators and diagrams to facilitate the understanding of model responses to emission changes when models are to be used for policy support. These indicators are shown to be useful to retrieve information on the magnitude of the locally produced impacts of emission reductions on concentrations with respect to the "external to the domain" contribution but also to identify, distinguish and quantify impacts arising from different factors (different precursors). In addition information about the robustness of the model results is provided. As such these indicators might reveal useful as first screening methodology to identify the feasibility of a given action as well as to prioritize the factors on which to act for an increased efficiency.

Finally all indicators are made dimensionless to facilitate the comparison of results obtained with different models, different resolutions, or on different geographical areas.

1. Introduction

Air quality models are useful tools for the assessment and forecast of pollutant concentrations in the atmosphere. With their increased use to support policy their evaluation becomes an important issue which is addressed in several documents published by policy-making authorities (EPA, 2007, 2009; Derwent et al., 2010; EEA, 2011; ASTM standard D6589, 2000). Most of the evaluation process relies on the "operational phase" or in other words the comparison of model results with available measurements which provides insight on the model capability to reproduce measured concentrations for a given application. Several statistical performance indicators (e.g. bias, correlation…) and diagrams (Jolliff et al., 2009; Taylor, 2001; Thunis et al., 2012, 2013) have been proposed to support the air quality modelers in this task.

But one of the key advantages of air quality models lies in their ability to assess the impact of precursor emission reductions on air quality levels. Models can then be used to support the design and the assessment of air quality plans by providing insight on the expected impacts of emission abatement measures on concentration levels (e.g. EMEP). Models are then used in a dynamic mode (i.e. response to a change in a given model input data) for which evaluation of the model performances becomes a challenge. This type of evaluation is one of the four steps (operational, diagnostic,

* Corresponding author.
E-mail address: philippe.thunis@jrc.ec.europa.eu (P. Thunis).

http://dx.doi.org/10.1016/j.atmosenv.2014.09.016

dynamic and probabilistic) included in the framework for evaluating regional scale numerical photochemical modeling systems proposed by Dennis et al. (2010). So far dynamic evaluation has not received as much attention as its operational counterpart despite the fact that air quality models are regularly applied in this mode for policy support. One of the reason is obviously the greater difficulty to perform this type of evaluation caused by the lack or incompleteness of measurement data.

The Forum for air quality modeling in Europe (Fairmode) guidance document (EEA, 2011) provides some methodological suggestions to perform dynamic evaluation: (1) assess the ability of the air quality model to reproduce historical pollution trends. This exercise brings valuable information on the model capability to react properly to emission changes but it often requires an intensive preparation work in terms of input data (e.g. preparation of past years emission inventories and consistent measurements) and has the drawback of mixing various factors in the analysis (e.g. both emissions and meteorology would change across the years investigated in the retrospective analysis). Examples of applications of this first methodology can be found in Napelenok et al. (2011), Gilliland et al. (2008), Godowitch et al. (2010) or Zhou et al. (2013); (2) assess the model ability to capture the main time variations within the simulated period (e.g. weekly, day–night and/or seasonal). By grouping all data into clusters (e.g. all week-end days within a year) meteorological conditions are mostly filtered out and the impact of emission changes can be more easily identified (Pierce et al., 2010). This methodology can be very useful to identify potential problems in the input data (e.g. emissions time profiles).

These two methodologies still rely on the availability of measurement data to test the dynamic response of the air quality models. One of the obvious methods to further pursue this dynamic evaluation process is to perform model inter-comparison exercises (referred to as probabilistic evaluation). Although no observation are available and therefore no comparison with the "truth" can be made this type of exercise proves to be extremely useful to flag out "strange" model behaviors but also to better understand the model behavior in general (e.g. Eurodelta (Thunis et al., 2010), Citydelta (Cuvelier et al., 2007; Thunis et al., 2007), AQMEII (Solazzo et al., 2012)).

In this work we propose a methodology to support this probabilistic evaluation process but specifically focusing on the dynamic aspects. Similarly to the approach presented in Thunis et al. (2012) for the operational evaluation of air quality models simple indicators and diagrams are developed to support the dynamic evaluation process. These indicators and diagrams aim at synthesizing in systematically information on key aspects of the model responses to emission changes that can be used for policy support.

The indicators proposed in this work aim at responding to the following three questions: (1) what is the impact of given emission precursor reductions in a given geographical area in quantitative terms (or in other words how much of the observed pollution levels originates from the domain of interest and how much from outside?), (2) what is the relative potency (ratio of the abated concentration and abated emissions) of a given precursor with respect to the others and (3) how robust are model responses to emission changes? These indicators are made dimensionless to facilitate their use across regions, models and allow meaningful inter-comparisons.

One of the main objectives of this work is to propose common indicators and diagrams to facilitate the understanding of model responses to emission changes when models are to be used for policy support.

The first section presents the concept and in particular the potencies which are the key element on which the indicators are constructed. In the second section the dynamic indicators are derived and detailed together with a summarizing diagram. The main advantages of these indicators and diagrams are then presented and the information which can be retrieved from them is discussed and examples shown.

2. Definition and concept

In this section the definitions and concepts required to construct the dynamic indicators and associated diagram are presented. These are based on the potency concept, i.e. a measure of the concentration change resulting from an emission reduction. We start with a simple situation in which the pollutant of interest depends only on a single emission precursor and then generalize this to the case in which many precursors have an impact on the pollutant concentration. In both cases a specific section is devoted to the separation of the linear and non-linear impacts since it is a key objective of this work to assess the degree of non-linearity and the robustness of the model responses to emission changes.

2.1. Potency for a single precursor

The **instantaneous potency** for a single pollutant l and precursor k, is defined as the local sensitivity (Yang et al., 1997) of the pollutant l to the emission of the precursor k, i.e. it is the infinitesimal concentration change at a specific location (for example a model grid-cell) resulting from an infinitesimal emission change of a precursor k over a given area A, or in mathematical terms:

$$\dot{P}^k = \frac{\mathrm{d}C}{\mathrm{d}E^k}$$

where

$\dot{P}^k = \dot{P}^{l,k}(x,y;A)$ is the instantaneous potency of pollutant l at the specific location (x, y) affected by the reduction of the precursor k emissions over the area A,

$C = C^l(x,y)$ is the concentration of pollutant l in grid-cell (x,y)

$E^k = E^k(A)$ are the precursor k emissions over the area A.

A finite emission change over the area A can be defined by using a reduction ratio α, as:

$$E^k - E^k_\alpha = \Delta E^k_\alpha = \alpha E^k$$

where $E^k_\alpha = E^k_\alpha(A)$ are the precursor k emissions over area A remaining after the emission reduction α

and $\Delta E^k_\alpha = \Delta E^k_\alpha(A)$ is the precursor k emission change over the area A.

For a finite emission change characterized by a ratio α we define an **average potency** (named potency in the following) as follows:

$$P^k_\alpha = \frac{\Delta C^k_\alpha}{\Delta E^k_\alpha} = \frac{\Delta C^k_\alpha}{\alpha E^k}$$

where $\Delta C^k_\alpha = \Delta C^k_\alpha(x,y) = C - C^k_\alpha$ is the concentration change in which $C^k_\alpha = C^{l,k}_\alpha(x,y)$ is the concentration resulting from the remaining emissions E^k_α

and $P^k_\alpha = \overline{P}^{l,k}_\alpha(x,y;A)$ is the potency.

Note that the same potency value can result from different combination of concentration and emission changes. Indeed a potency of 0.5 can either result from a concentration change of 10

(concentration unit) and an emission change of 20 (emission unit) or from a concentration change of 2 (concentration unit) and associated emission change of 4 (emission unit).

Note also that in the case of PM_{10} for which concentration is measured in units of $\mu g/m^3$ the potency would be expressed as an inversed average speed (s/m).

2.2. Relative potency for a single precursor

As the values obtained for the above defined average potency are in theory unbounded, we introduce in this section the relative potency with the view to construct a dimensionless indicator.

The **relative potency** $p_\alpha^k = \overline{p}_\alpha^{l,k}(x,y;A)$ is defined relatively to a reference as follows:

$$p_\alpha^k = \frac{P_\alpha^k}{P_{\text{full}}^k} \text{ where } p_{\text{full}}^k = \frac{C}{E^k} \text{ is the } \textbf{full potency}.$$

According to this definition, the relative potency is equal to unity when the potency is equal to the full potency, i.e. when a full emission reduction ($\alpha = 1$) produces a full reduction of concentration ($\Delta C_\alpha^k = C$).

Given the above relations, the relative potency can be expressed as:

$$p_\alpha^k = \frac{\Delta C_\alpha^k}{\alpha C}$$

One advantage of this relative formulation resides in the fact that relative potencies are constructed on the basis of concentration values only whereas average potencies require explicit information on emissions. Similarly to the absolute potency, the same relative potency value can result from different combination of concentration and emission percentage changes. Indeed a potency of 0.5 can either result from a concentration change of 10% and an emission change of 20% or from a concentration change of 2% and associated emission change of 4%.

Another advantage of the relative formulation is the fact that it is quasi-bounded. The relative potency is indeed equal to 0 when the potency is itself 0 (i.e. the emission change does not produce any effect on the concentration) and is equal to 1when a full emission reduction produces a full concentration reduction. An intermediate value, e.g. 0.5 then means that an emission reduction of α would lead to a reduction of the concentration levels of 0.5α. It can however also be negative when a reduction of emissions leads to an increase of concentration. Consequently, even if the values of the relative potencies are not completely bounded on the negative side, they are expected to remain between -1 and 1 in most situations.

2.3. Linear change and robustness of the potency for a single precursor

Potencies are simple indicators which can serve as useful instrument for decision making. But potencies are computed on the basis of one specific emission reduction ratio and their usefulness depends on the possibility to use them for other reduction ratios that for the one used to compute them. In other words potencies should be robust, i.e. remain close to a constant value over a certain range of emission reduction levels around the one selected to compute them. We propose in this section a formulation to quantify this robustness.

The robustness of the average and relative potencies is directly linked to the linearity of the concentration change with the emission change. To illustrate this point, we split the concentration change into its linear and non-linear components for a given reduction ratio α between 0 and a reference level β as follows:

$$\Delta C_\alpha^k = \Delta C_\alpha^{k,\text{lin}} + \Delta C_\alpha^{k,\text{nlin}}$$

The linear change of concentration can be defined with respect to the reference emission reduction ratio β as:

$$\Delta C_\alpha^{k,\text{lin}} = \frac{\alpha}{\beta}\Delta C_\beta^k$$

Consequently, the potency can also be split into its linear and non-linear components:

$$P_\alpha^k = P_\alpha^{k,\text{lin}} + P_\alpha^{k,\text{nlin}} \text{ and } p_\alpha^k = p_\alpha^{k,\text{lin}} + p_\alpha^{k,\text{nlin}}$$

And it is easy to show that the linear component of the potencies remains constant for any reduction ratio:

$$P_\alpha^{k,\text{lin}} = P_\beta^k \text{ and } p_\alpha^{k,\text{lin}} = p_\beta^k \text{ for any } \alpha.$$

The potencies will therefore be robust (i.e. quasi-constant over a range of emission reduction ratios) when the non-linear term can be neglected with respect to the linear term.

Before using these definitions and concepts to construct a summarizing diagram we extend the potency approach to the case in which the pollutant concentration depends on more than one precursor.

2.4. Potency for several precursors

The **potency** for a single pollutant l and several precursors k is defined as the concentration change at a specific location (for example a model grid-cell) resulting from an emission change of a series of precursor k over a given area A, or in mathematical terms:

$$P_\alpha^{\{k\}} = \frac{\Delta C_\alpha^{\{k\}}}{\Delta E^*} = \frac{\Delta C_\alpha^{\{k\}}}{\alpha E^*}$$

where

$P_\alpha^{\{k\}}$ is the potency resulting from the change of several precursor emissions, each reduced by the same reduction ratio α.
ΔE^* is an **equi-potency emission change**.

The equi-potency emission change is calculated by applying the factor separation methodology of Stein and Alpert (1993) to both the concentration change and to the potency as follows:

- First the concentration change is split as:

$$\Delta C_\alpha^{\{k\}} = \sum_k \Delta C_\alpha^k + \Delta C_\alpha^{\text{int}}$$

where $\sum_k \Delta C_\alpha^k$ is the sum of the concentration changes resulting from the precursors emission changes one by one.

$\Delta C_\alpha^{\text{int}}$ is the concentration change resulting from the interaction between the different precursors.

- Second the potency is split in a similar way:

$$P_\alpha^{\{k\}} = \sum_k P_\alpha^k + P_\alpha^{\text{int}}$$

where P_α^k are the potencies for the single precursor k and P_α^{int} the potency resulting from the interaction among precursors.

Dividing the first relation by ΔE^* we get: $P_\alpha^{\{k\}} = \frac{\sum_k \Delta C_\alpha^k}{\Delta E^*} + P_\alpha^{\text{int}}$.

Comparing this last relation with the potency equality, we then obtain an expression for the sum of the single precursor potencies: $\sum_k P_\alpha^k = \frac{\sum_k \Delta C_\alpha^k}{\Delta E^*}$.

It is then possible to get: $\Delta E^* = \frac{\sum_k \Delta C_\alpha^k}{\sum_k \Delta C_\alpha^k / \Delta E_\alpha^k} = \frac{\sum_k P_\alpha^k \Delta E_\alpha^k}{\sum_k P_\alpha^k}$.

This definition of ΔE^* ensures that the Stein and Alpert decomposition can be amply in coherent way for the concentration changes as well as for the potencies.

Note that if the emission reduction of a specific precursor k does not lead to any concentration variation ($\Delta C_\alpha^k = 0$) it does not affect the calculation of ΔE^* and consequently of the potency.

2.5. Relative potency for several precursors

A similar approach can be used for the relative potency in the case of a multiple precursors emission reduction:

$$p_\alpha^{\{k\}} = \frac{\Delta C_\alpha^{\{k\}}}{\alpha C}$$

where α is the single emission reduction ratio applied to all precursor emissions.

Similarly to the proposed separation into single and interaction impacts for the potency (above section), we also decompose the relative potency in similar terms:

$$p_\alpha^{\{k\}} = \sum_k p_\alpha^k + p_\alpha^{\text{int}}$$

2.6. Linear change and robustness for several precursors

Similarly to the case of a single precursor, the robustness of the potencies for several precursors is linked to the linear change of the concentration. When the linear and non-linear components of the single precursor potencies are introduced in the Stein and Alpert (1993) decomposition it gives:

$$P_\alpha^{\{k\}} = \sum_k P_\alpha^{k,\text{lin}} + \sum_k P_\alpha^{k,\text{nlin}} + P_\alpha^{\text{int}}$$

However, we have seen that, for a single precursor k, a linear change of concentration can be defined using two abatement ratios α and β, β being a reference reduction level and α any reduction level between 0 and β, then:

$$P_\alpha^{k,\text{lin}} = P_\beta^k \text{ for any } \alpha.$$

The potency can also be written for the reference reduction level β using the Stein and Alpert (1993) decomposition:

$$P_\beta^{\{k\}} = \sum_k P_\beta^k + P_\beta^{\text{int}}$$

Note that this relation does not distinguish linear and non-linear components as these are defined only with respect to the reference case.

The potency is robust if $P_\alpha^{\{k\}}$ is close to $P_\beta^{\{k\}}$ for any α. This condition is equivalent to say that $\sum_k P_\alpha^{k,\text{nlin}} + P_\alpha^{\text{int}} - P_\beta^{\text{int}}$ is small with regards to $P_\alpha^{\{k\}}$.

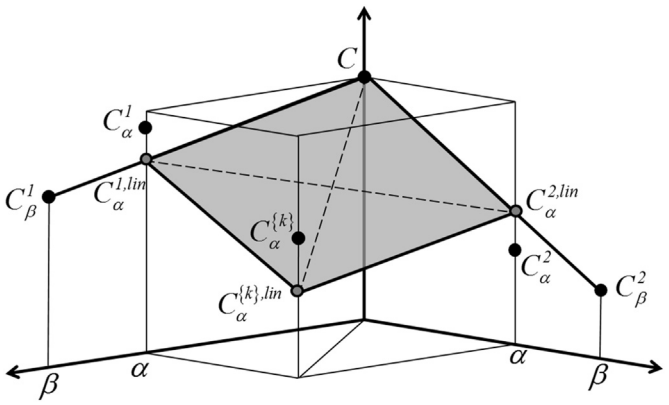

Fig. 1. Reduction levels due to the reduction of two precursors. Concentration levels are plotted on the vertical axis and the precursor reductions on the horizontal axis. There are two levels of reductions on each horizontal axis (α, β; β being the reference reduction level). The model response is linear if $C_\alpha^{\{k\}} = C_\alpha^{\{k\},\text{lin}}$ with $C_\alpha^{\{k\},\text{lin}}$ being a multi-linear interpolation of C, $C_\alpha^{1,\text{lin}}$ and $C_\alpha^{2,\text{lin}}$ (i.e. C, $C_\alpha^{1,\text{lin}}$, $C_\alpha^{2,\text{lin}}$ and $C_\alpha^{\{k\},\text{lin}}$ are in a common plane). Linearity of the answer implies two conditions: 1) $C_\alpha^{1,\text{lin}}$ (resp. $C_\alpha^{2,\text{lin}}$) is a linear interpolation of C andC_β^1 (resp. C and C_β^2) then $p_\alpha^{1,\text{lin}} = p_\beta^1$ (resp. $p_\alpha^{2,\text{lin}} = p_\beta^2$). 2) There is no interaction between the precursors: $\Delta C_\alpha^{\text{int}} = 0$ then $p_\alpha^{\text{int}} = 0$. Consequently, it results from these two conditions that $p_\alpha^{\{k\},\text{lin}} = p_\beta^1 + p_\beta^2$.

It is interesting to note that the potency for several precursors is robust when the concentration change can be assumed linear. Indeed, in such situation $P_\alpha^{\text{int}} \approx P_\beta^{\text{int}} \approx 0$ and $P_\alpha^{k,\text{nlin}} \approx 0$. But the robustness can also result from compensation among the 3 terms. For example when the interaction terms are the same for different reduction levels, (i.e. $P_\alpha^{\text{int}} \approx P_\beta^{\text{int}}$) and when the concentration changes resulting from the single precursor reductions are quasi linear, (i.e. $P_\alpha^{k,\text{nlin}} \approx 0$).

3. A practical application

3.1. Scenario procedure

In the present work we propose indicators that provide information about the effect of emission reductions on the concentrations. These indicators are based on the concentration changes obtained with a series of independent simulations in which the emissions of the different precursors are reduced independently. If we take the example of PM_{10} concentrations they result from the emissions of different precursors: NO_x, SO_2, VOC, NH_3 and primary particulate matter (PPM). A chemistry transport air quality model can therefore be used to perform a series of simulations over a geographical domain reducing the precursor emission over a given area included into the calculation domain. The number of requested simulations is equal to $2 \times n + 3$ where n is the number of input parameters to be tested. With 5 emission precursors like in our example, the following thirteen simulations need to be performed:

- A base case simulation which will provide base case PM_{10} concentrations, referred with the symbol C in the following.
- One simulation with a reference level (β) emission reduction of a single precursor k (NH_3, NO_x, SO_2, VOC and PPM). This run is repeated for the 5 precursors to lead to reduced concentrations referred to as C_β^k. In the current work all β have been set to 50%. This level represents a compromise between (1) a large enough reduction to capture the main aspects of the model responses to significant changes in the input data and (2) a level of reduction which remains realistically achievable in terms of human activity constraints and prevents the appearance of strange model

behaviors (e.g. responses of models used in extreme parameter ranges)

- One simulation with a variable level ($\alpha < \beta$) emission reduction of a single precursor k (NH_3, NO_x, SO_2, VOC and PPM). This run is repeated for the 5 precursors to lead to reduced concentrations referred to as C_α^k. In the current work all α have been set to 20%.
- Two simulations in which all 5 precursor emissions are reduced contemporarily by α and β, respectively. This will lead to concentration levels referred to as $C_\alpha^{\{k\}}$ and $C_\beta^{\{k\}}$.

Fig. 1 shows graphically in a three-dimensional space the different level of reduction that the two precursors can achieve. Note that the proposed methodology is applied here to analyze and distinguish the impact of different emission precursors on concentration levels but it could also be applied to distinguish the impacts of different emission sectors (e.g. the 11 CORINAIR SNAP macro-sectors requiring then a set of 25 simulations) or other interacting set of parameters. The proposed methodology aims at screening averaged potencies calculated between two levels of reduction: α and β. The estimation of non-linearity is relative to these averages. Additional simulations might be needed to capture stronger non-linearities as was done for example by Wang et al. (2011) to assess the non-linearities of specific species involved in the formation of inorganic aerosols.

3.2. Indicators

A series of indicators are constructed, based on the potencies defined above to provide information about the concentration changes resulting from emission changes.

The first indicators are the relative potencies defined previously for the single and multiple precursor emission reductions:

$$I_\alpha^k = p_\alpha^k \text{ and } I_\alpha^{\{k\}} = p_\alpha^{\{k\}}$$

Another indicator $I^{\max}$ is constructed to provide information about the maximum concentration change resulting from an emission reduction. This maximum impact might result from either a combined reduction of all precursors or through the reduction of one single precursor if different precursors lead to opposite impacts and tend to counter-balance each other. $I^{\max}$ is therefore equal to the maximum among $I_\alpha^{\{k\}}$ and the series of individual I_α^k. Since an emission precursor reduction does not always lead to a concentration reduction (e.g. a reduction of NO_x emissions might lead to an increase of the O_3 concentrations in a VOC limited environment) I_α^k or $I_\alpha^{\{k\}}$ can be positive as well as negative. As we are interested to capture the maximum impact, regardless of its sign, we use as indicator the absolute value of $I^{\max}$ which can be estimated from the different simulations described previously and is formulated as follows:

$$|I^{\max}| = \max\left[\left|p^{\min}\right|, \left|p^{\max}\right|\right]$$

where $p^{\max}$ and $p^{\min}$ are the maximum and minimum average relative potencies differences expressed as:

$$p^{\max} = \max\left[\left\{p_\alpha^k\right\}, p_\alpha^{\{k\}}\right] \text{ and } p^{\min} = \min\left[\left\{p_\alpha^k\right\}, p_\alpha^{\{k\}}\right]$$

The sign of the maximum concentration deviation is then introduced using the parameter ε equal to 1 when $|p^{\min}| \le |p^{\max}|$ and -1 when $|p^{\min}| > |p^{\max}|$.

Finally, $I^{\max} = \varepsilon |I^{\max}|$.

In general, $I^{\max}$ is equal to $I_\alpha^{\{k\}}$ but it can occasionally be equal to I_α^k if the effect of reducing one precursor alone is more important than the effect of the simultaneous reduction of all precursors.

This indicator can reach 0 meaning that emission reductions have no impact on the concentrations levels observed within the domain of interest (background impacts strongly dominates), be close to 1 when emission reductions are fully effective and reduce concentration levels in the same proportion as emission reductions but can also be negative when overall emission reductions lead to a concentration increase. Note that this indicator is based on an emission reduction of all precursors contemporarily and is therefore common to all precursors. As mentioned above the emission reduction level β is meant as a reference level around which the model behavior is analyzed. As mentioned earlier this level is here set to 50%.

A last indicator (J_α^k) provides information on the importance of a given single precursor impact in terms of concentration change relatively to the others. It is formulated as:

$$J_\alpha^k = \frac{I_\alpha^k}{|I^{\max}|}$$

This indicator ranges between 0 (no impact) and 1 (full impact) with negative values indicating concentration increases resulting from the given precursor emission decrease.

3.3. Diagram

The two previously described indicators ($I^{\max}$ and J_α^k) are used as abscissa and ordinates to construct a diagram summarizing the different aspects (precursor emission impact, robustness…) presented in the first section (Fig. 2). These different aspects are detailed below individually. We recall here that emissions are reduced in a given local geographical area (A) while the impact of these emission reductions is evaluated at each location (e.g. grid cells). In the diagram each point (blue circle) represents a particular location or grid cell. One similar diagram is constructed for each precursor impacting the concentration and deliver the following information.

3.3.1. Local vs. boundary impact

This information is directly provided on the X-axis by the indicator $I^{\max}$ which provides a quantitative estimate of the maximum impact that local (over the selected domain A) emission reductions have on concentration levels. As an example a value of -0.5 for this indicator $I^{\max}$ means that a reduction of 100% of all emission precursors together or single precursor emission reductions would lead at maximum to a 50% change of the concentration levels, meaning that the remaining 50% originate from processes that are

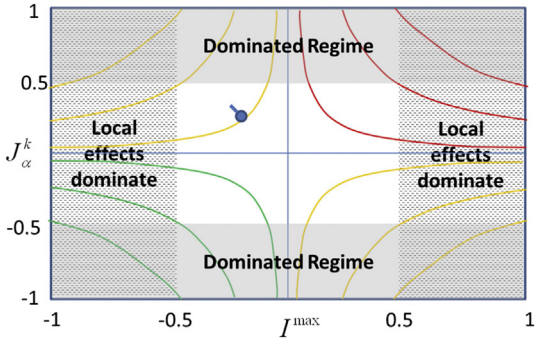

Fig. 2. Schematic potency diagram indicating the main zones of interest. The X axis provides information of the local vs. boundary contribution to air pollution whereas the Y axis gives a relative estimate of the impact of one precursor against the others. For more details about the different zones highlighted in this diagram, the reader is referred to Section 3 (diagram subsection).

out of control locally (boundary conditions, natural emissions…). The absolute value of 0.5 has been chosen in this diagram (dashed shaded area) to indicate this frontier between locally and boundary dominated impacts. As mentioned a precursor or a multi-precursor emission reduction can also lead to a positive impact, meaning that concentration levels would rise in response to an emission reduction. Grid cells experiencing this behavior would be located on the right side of the diagram. As mentioned above one specific diagram is constructed for each precursor having an impact on the selected pollutant but the I^{max} indicator represents the maximum of all impacts (combined and individual) and remains therefore similar for all diagrams for a given pollutant.

3.3.2. Precursor vs. precursor impact

On the ordinate axis the indicator J_α^k is constructed as the ratio of the potency of a given precursor over the maximum overall impact. Although the maximum impact is not always the sum of the individual impacts due to non-linearities, the vertical axis can be used to estimate the potency of one precursor against another by comparing the position of a given point in the various precursor diagram for a given pollutant. Similarly to the local vs. boundary impact a delimitation line at 0.5 and −0.5 has been inserted (dashed areas) to indicate the predominant impact of the given precursor with respect to others. The indicator J_α^k can have values ranging from −1 to 1 to reflect the fact that the impact of one specific precursor can either be positive (increase of concentration as a result of an emission reduction) or negative (decrease of concentration as a result of an emission reduction).

3.3.3. Precursor impact on concentration levels

If they are multiplied, the two indicators I^{max} and J_α^k gives I_α^k which provides information on the percentage impact of a single precursor (the one associated to the diagram) on the selected pollutant concentration. This information is given by the hyperbolas which represent precursor impacts of 5%, 25% and 50%, starting from the origin point outwards, respectively. In summary the *X* axis provides information on the overall maximum impact (combined or single precursor emission reductions), the *Y* axis informs on the relative importance of one precursor with respect to the others while the hyperbolas inform on the quantitative impact of this precursor. The area contained within the first hyperbolas can directly be associated to very weak impacts of the given precursor on concentration levels.

3.3.4. Robustness

The indicators I^{max} and J^k are calculated for two different levels of emission reduction (α and β). This information is included in the diagram by drawing a line (line attached to the circle) that links the position obtained for the reference reduction (β-circle) to the position that would be obtained in the case of the smaller emission reduction (α). These lines directly inform on the degree of robustness of the model responses. In the case of small lines or in the case of not-negligible lines but contained in a low impact zone (i.e. within the area delimited by the first hyperbolas) the solution can be considered as robust.

3.3.5. Additional information

1) This diagram can be used to provide information on the relative and absolute importance of different factors. In this work the focus has been on the analysis of different emission precursors but the same analysis might be performed for other aspects, e.g. emission macro-sectors. In this case however the requested scenario simulations would change but the same principles would hold.
2) As each point in the diagram represents a grid cell, a color scheme can be used to identify different cluster of points (e.g. high vs. low percentile concentration levels, urban vs. rural, geographical areas…) and provide additional information.
3) In given case specific situations can be delimitated in the diagram. In the particular case of O_3 concentrations (Fig. 3 (left) which shows the impact of VOC emissions on O_3) which are mostly influenced by two emission precursors (NO_x and VOC), the characteristic NO_x-limited and VOC-limited chemical regimes which correspond to regimes where one of the two precursor emission dominates the other (Sillman, 1999) are easily derived and correspond to well identified zones in the diagram. The VOC limited regime is further split into two possible modes: O_3 increases or decreases (bottom right and left parts of the diagram). Note that some parts of the diagrams can correspond to impossible impacts (in this particular case VOC emission reduction would not result in increases of O_3 concentrations) and are represented with gray shading. A similar diagram is produced for the impacts of NO_x on PM_{10} concentrations (Fig. 3 (right)). As PM_{10} concentrations are sensible to more precursor than O_3 (i.e. NO_x, VOC, PPM, SO_2 and NH_3) it is not possible to identify as many zones as for O_3 but the same logic holds.

3.3.6. Practical example

In this section we describe the application of the proposed methodology to a practical example. To this purpose we use a series of model simulations performed in one region in Europe. As the goal is to illustrate in how the proposed indicators and diagram can be used in a practical case, we will not provide details about the model selected, its setup and the location over which the emission reductions have been performed. Thirteen simulations corresponding to the ones described in the scenario section above have been performed to produce the diagram in Fig. 4. Although 5 precursors have been reduced in these runs we focus here on PM_{10} concentrations resulting from NO_x and SO_x only for the analysis. In these figures (top ones) each point represents a grid cell concentration which color is proportional to the concentration value (red for the 20th highest percentile, blue for the 20th lowest percentile and green in between). From these two figures, one notice that the maximum impact (*x* axis) is about 0.5 meaning that half of the concentration levels cannot be abated with local measures. Control measures are much more effective on NO_x than on SO_x. For NO_x the impact reaches about 20% for some grid cells (hyperbola) while for SO_x all grid locations have an impact below or close to 5%. It is also interesting to see that the maximum NO_x impact is not for the highest concentrations but rather for the middle range ones. Non-linearities are relatively weak and for this reason the bars are represented in a separate figure (bottom ones). The model responses to both NO_x and SO_2 emission reductions can be considered as linear, meaning that the uncertainty on the level of the decided abatement level will have little impact on the conclusion (robust decision making).

It is important to note that the proposed diagram is dimensionless and can provide information comparable across models even though the reduction level β differs from one case to the other. A similar diagram could be constructed but using the average absolute potencies in place of the relative potencies. In this case the diagram is not bounded anymore but can be used to retrieve information on the magnitude of the potency and offer a reference comparison point among models and regions. It is important to note that while the indicators based on relative potencies depend on the emission inventory precursor distribution (i.e. the relative potency of one precursor also depends on the proportion of this

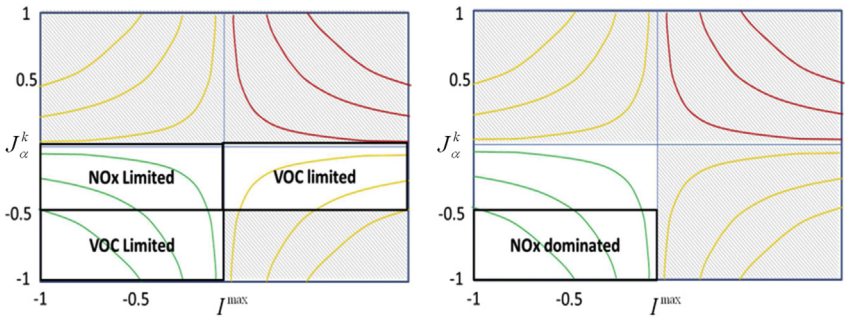

Fig. 3. Same as Fig. 2 but the zones in the diagram are specific to Ozone (left) and its dependency on VOC. The different chemical regimes identified by Sillman (1999) are highlighted. For more details the reader is referred to Section 3 (subsection additional information). On the right the same approach is followed for the impact of NO_x emission reduction on PM_{10}. Gray shaded areas represent impossible (or improbable) model responses.

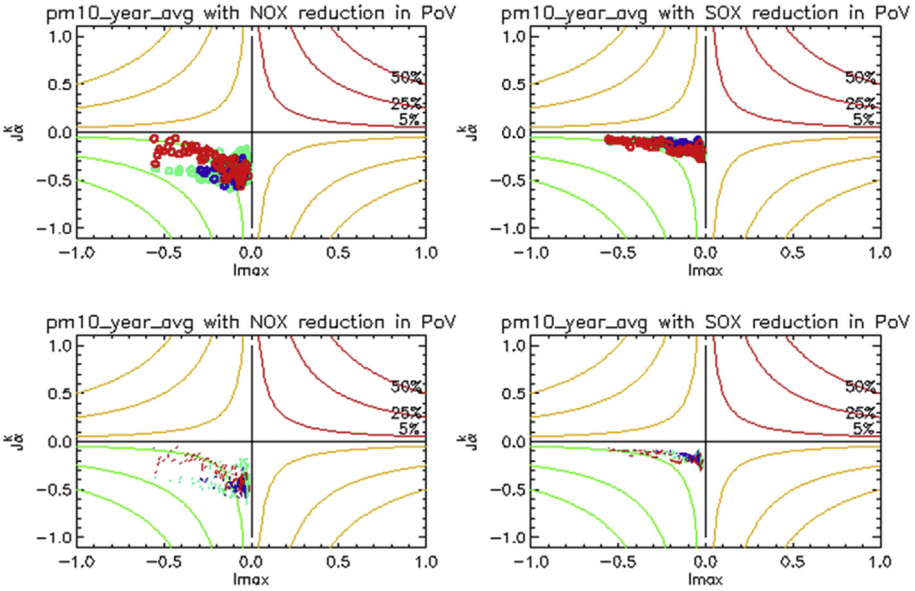

Fig. 4. The potency diagram is used on the specific case of PM_{10} which depends on 5 different precursors. NO_x and SO_x impacts are illustrated here. Each point corresponds to a specific grid cell and the color scheme is related to the PM_{10} concentration value (20th upper percentile in red, 20th lower percentile in blue, and green in between). In the bottom two diagrams, the lines relating the results obtained with two different emissions abatement ratios are shown. They are indicative of the robustness of the model responses. (For interpretation of the references to color in this figure legend, the reader is referred to the web version of this article.)

precursor emission in the inventory), this is not the case for the average absolute potencies. The two types of diagrams serve therefore different purposes.

4. Conclusions

In this work indicators and diagrams to support the evaluation of models used in a dynamic mode have been presented and discussed. Indeed models are regularly used in a dynamic mode to assess the impact of emission reductions on air quality concentrations. In such case observations cannot be used for the assessment and other methods must be used.

These indicators are shown to be useful to retrieve information on the magnitude of the locally produced impacts of emission reductions on concentrations with respect to the "external to the domain" contribution but also to identify, distinguish and quantify impacts arising from different factors (different precursors). In addition information about the robustness of the model results is provided. As such these indicators might reveal useful as first screening methodology to identify the feasibility of a given action as well as to prioritize the factors on which to act for an increased efficiency.

Finally all indicators are made dimensionless to facilitate the comparison of results obtained with different models, different resolutions, or on different geographical areas.

The analysis can be generalized to any given set of parameters and could be extended as well to other fields in which a variable results from complex interactions among a set of input parameters.

Acknowledgments

None declared.

Annex. Extension of the multi-precursor potencies approach to variable emission reduction levels

So far potencies for multiple precursors have been defined for the particular case of a constant reduction ratio α (same reduction level applied to all precursors). This concept can be extended for reductions ratios α_k which are different for each precursor k.

Potency for several precursors

Using different reduction ratios α_k, the potency resulting for several precursor emission changes can be written as follows:

$$P_{\alpha_k}^{\{k\}} = \frac{\Delta C_{\alpha_k}^{\{k\}}}{\Delta E^*}$$

where ΔE^* is an equi-potency emission change defined as the weighed combination of the emission changes of each precursor:

$$\Delta E^* = \frac{\sum_k P_{\alpha_k}^k \Delta E_{\alpha_k}^k}{\sum_k P_{\alpha_k}^k}$$

Relative potency for several precursors

The extension for the relative potencies gives:

$$p_{\alpha_k}^{\{k\}} = \frac{\Delta C_{\alpha_k}^{\{k\}}}{\alpha^* C}$$

with α^* an equi-potency emission reduction ratio defined similarly to the equi-potency emission change ΔE^* but with relative potency as weighting factors.

$$\alpha^* = \frac{\sum_k p_{\alpha_k}^k \alpha_k}{\sum_k p_{\alpha_k}^k}$$

We note that the expression of the equi-potency emission reduction ΔE^* and the equi-potency emission ratio α^* guarantees that the multi-precursor potency and relative potency can be split using the Stein and Alpert decomposition:

$$P_{\alpha_k}^{\{k\}} = \sum_k P_{\alpha_k}^k + P_{\alpha_k}^{\text{int}} \text{ and } p_{\alpha_k}^{\{k\}} = \sum_k p_{\alpha_k}^k + p_{\alpha_k}^{\text{int}}$$

Decomposition which can be extended to show all the non-linear terms:

$$P_{\alpha_k}^{\{k\}} = \sum_k P_{\alpha_k}^{k,\text{lin}} + \sum_k P_{\alpha_k}^{k,\text{nlin}} + P_{\alpha_k}^{\text{int}} \text{ and } p_{\alpha_k}^{\{k\}} = \sum_k p_{\alpha_k}^{k,\text{lin}} + \sum_k p_{\alpha_k}^{k,\text{nlin}} + p_{\alpha_k}^{\text{int}}$$

Finally the **equi-potential emissions** E^* can be defined starting from ΔE^* and α^*:

$$E^* = \frac{\Delta E^*}{\alpha^*}$$

It can be shown that these equi-potential emissions can be written as a weighed combination of the emissions of each precursor with weights given by the single precursor potencies:

$$E^* = \frac{\sum_k P_{\alpha_k}^k E_k}{\sum_k P_{\alpha_k}^k}$$

References

ASTM, 2000. Standard Guide for Statistical Evaluation of Atmospheric Dispersion Model Performance. D6589-00. American Society for Testing and Materials, West Conshohocken, PA.

Cuvelier, C., Thunis, P., Vautard, R., Amann, M., Bessagnet, B., Bedogni, M., Berkowicz, R., Brandt, J., Brocheton, F., Builtjes, P., Carnavale, C., Coppalle, A., Denby, B., Douros, J., Graf, A., Hellmuth, O., Hodzic, A., Honore, C., Jonson, J., Kerschbaumer, A., de Leeuw, F., Minguzzi, E., Moussiopoulos, N., Pertot, C., Peuch, V.H., Pirovano, G., Rouil, L., Sauter, F., Schaap, M., Stern, R., Tarrason, L., Vignati, E., Volta, M., White, L., Wind, P., Zuber, A., 2007. CityDelta: a model intercomparison study to explore the impact of emission reductions in European cities in 2010. Atmos. Environ. 41, 189–207.

Dennis, R., Fox, T., Fuentes, M., Gilliland, A., Hanna, S., Hogrefe, C., Irwin, J., Rao, S.T., Scheffe, R., Schere, K., Steyn, D., Venkatram, A., 2010. A framework for evaluating regional scale numerical photochemical modeling systems. Environ. Fluid Mech. 10, 471–489.

Derwent, D., Fraser, A., Abbott, J., Willis, P., Murrells, T., 2010. Evaluating the Performance of Air Quality Models (No. Issue 3). Department for Environment and Rural Affairs.

EEA (European Environment Agency), The Application of Models Under the European Union's Air Quality Directive: A Technical Reference Guide, EEA Technical Report No 10/2011.

EPA (U.S. Environmental Protection Agency), 2007. Guidance on the Use of Models and Other Analyses for Demonstrating Attainment of Air Quality Goals for Ozone, $PM_{2.5}$, and Regional Haze. EPA-454/B-07-002. http://www.epa.gov/scram001/guidance/guide/final-03-pm-rh-guidance.pdf.

EPA (U.S. Environmental Protection Agency), 2009. Guidance Document on the Development, Evaluation, and Application of Regulatory Environmental Models. EPA-HQ-ORD-2009. http://www.epa.gov/crem/library/cred_guidance_0309.pdf.

Gilliland, A.B., Hogrefe, C., Pinder, R.W., Godowitch, J.M., Foley, K.L., Rao, S.T., 2008. Dynamic evaluation of regional air quality models: assessing changes in O_3 stemming from changes in emissions and meteorology. Atmos. Environ. 42, 5110–5123.

Godowitch, J.M., Pouliot, G.A., Rao, S.T., 2010. Assessing multi-year changes in modeled and observed urban NO_x concentrations from a dynamic model evaluation perspective. Atmos. Environ. 44, 2894–2901.

Jolliff, J.K., Kindle, J.C., Shulman, I., Penta, B., Friedrichs, M.A.M., Helber, R., Arnone, R.A., 2009. Summary diagrams for coupled hydrodynamic-ecosystem model skill assessment. J. Mar. Syst. 76, 64–82.

Napelenok, S.L., Foley, K.M., Kang, D., Mathur, R., Pierce, T., Rao, S.T., 2011. Dynamic evaluation of regional air quality model's response to emission reductions in the presence of uncertain emission inventories. Atmos. Environ. 45, 4091–4098.

Pierce, T., Hogrefe, C., Trivikrama Rao, S., Steven Porter, P., Ku, J.Y., 2010. Dynamic evaluation of a regional air quality model: assessing the emissions-induced weekly ozone cycle. Atmos. Environ. 44, 3583–3596.

Sillman, S., 1999. The relation between ozone, NO_x and hydrocarbons in urban and polluted rural environments. Atmos. Environ. 33, 1821–1845.

Solazzo, E., Bianconi, R., Vautard, R., Appel, K.W., Moran, M.D., Hogrefe, C., Bessagnet, B., Brandt, J., Christensen, J.H., Chemel, C., Coll, I., Denier van der Gon, H., Ferreira, J., Forkel, R., Francis, X.V., Grell, G., Grossi, P., Hansen, A.B., Jericevic, A., Kraljevic, L., Miranda, A., Nopmongcol, U., Pirovano, G., Prank, M., Riccio, A., Sartelet, K.N., Schaap, M., Silver, J.D., Sokhi, R.S., Viras, J., Werhahn, J., Wolke, R., Yarwood, G., Zhang, J., Rao, S.T., Galmarini, S., 2012. Model evaluation and ensemble modelling of surface-level ozone in Europe and North America in the context of AQMEII. Atmos. Environ. 53, 60–74.

Stein, U., Alpert, P., 1993. Factor separation in numerical simulations. J. Atmos. Sci. 50, 2107–2115.

Taylor, K.E., 2001. Summarizing multiple aspects of model performance in a single diagram. J. Geophys. Res. 106, 7183–7192.

Thunis, P., Rouïl, L., Cuvelier, C., Stern, R., Kerschbaumer, A., Bessagnet, B., Schaap, M., Builtjes, P., Tarrason, L., Douros, J., Moussiopoulos, N., Pirovano, G., Bedogni, M., 2007. Analysis of model responses to emission-reduction scenarios within the CityDelta project. Atmos. Environ. 41, 208–220.

Thunis, P., Cuvelier, C., Roberts, P., While, L., Nyirni, A., Stern, R., Kerschbaumer, A., Bessagnet, B., Bergstroem, R., Schaap, M., 2010. EURODELTA – Evaluation of a Sectoral Approach to Integrated Assessment Modeling – Second Report. JRC – EUR 24474 EN.

Thunis, P., Pederzoli, A., Pernigotti, D., 2012. Performance criteria to evaluate air quality modeling applications. Atmos. Environ. 59, 476–482.

Thunis, P., Pernigotti, D., Gerboles, M., Belis, C., 2013. Model quality objectives based on measurement uncertainty. Part I: O_3. Atmos. Environ. 79, 861–868.

Wang, S., Xing, J., Jang, C., Zhu, Y., Fu, J.S., Hao, Jiming, 2011. Impact assessment of ammonia emissions on inorganic aerosols in East China using response surface modeling technique. Environ. Sci. Technol. 45, 9293–9300.

Yang, Y.J., Wilkinson, J.G., Russel, A.G., 1997. Fast, direct analysis of multidimensional photochemical models. Environ. Sci. Technol. 31, 2859–2868.

Zhou, W., Cohan, D.S., Napelenok, S.L., 2013. Reconciling NO_x emissions reductions and ozone trends in the U.S., 2002–2006. Atmos. Environ. 70, 236–244.